Dynamic Scaling of Cluster-Mass Distributions in Kinetic Colloid Aggregation

D. A. Weitz and M. Y. Lin[a]
Exxon Research and Engineering Company, Annandale, New Jersey 08801
(Received 2 December 1985)

The cluster-mass distributions produced in the kinetic aggregation of aqueous gold colloids are measured over an extended range of masses for two limiting kinetic regimes, diffusion-limited (DLA) and reaction-limited (RLA) aggregation. Markedly different distributions are found, with DLA having a peaked distribution, while RLA has a power-law distribution. In both cases the distributions are shown to exhibit dynamic scaling, as has recently been predicted. The data are interpreted with the Smoluchowski equations, and are used to determine the form of the appropriate kernel for each regime.

PACS numbers: 64.60.−i, 05.40.+j, 64.75.+g, 82.70.Dd

The study of the kinetic aggregation of small particles to form larger clusters has achieved new prominence[1,2] with the discovery that the structures of colloidal aggregates exhibit dilation symmetry, and thus are well described as fractals.[3,4] In an effort to develop a more fundamental understanding of these kinetic growth processes, attention has now turned to the dynamics, which are intrinsically related to the resultant structures. These dynamics are most clearly embodied in the cluster-mass distribution $N(m)$ and its time dependence. The shape of the cluster-mass distribution has a profound effect in determining the dominant reaction events which ultimately strongly influence the structure of the resultant clusters. Furthermore, it now appears that cluster-cluster aggregation can fall into two distinct regimes of behavior, each belonging to a separate universality class.[5-7] Knowledge of the cluster-mass distribution is crucial both to distinguish and identify each regime, and to develop any fundamental understanding of the kinetic behavior characterizing that regime. Finally, since many studies of colloid aggregation rely on scattering measurements, a knowledge of $N(m)$ is indispensable for proper interpretation of the results.

A convenient and widely used description of the cluster-mass distribution is through the use of the generalized Smoluchowski equations.[8-11] While these equations themselves cannot predict the shape of the aggregates, the effects of the structure, as well as most of the other important physics of the aggregation process, must be included in the kernel or reaction matrix used in their solution. It has recently been demonstrated that the solutions for a broad class of commonly encountered kernels exhibit a dynamic scaling[12,13] and can be classified into three general categories,[11] thus providing an important framework for the description of the aggregation dynamics. However, the key to the successful application of the Smoluchowski equations is the choice of the appropriate kernel, and this has been severely hampered by the lack of experimental data.

In this Letter, we present measurements of the cluster-mass distribution $N(m)$ and its time dependence, produced by the kinetic aggregation of aqueous gold colloids, and show that the shape of the cluster-mass distribution depends critically on the aggregation kinetics. We study two limiting kinetic regimes,[5] diffusion-limited (DLA) and reaction-limited (RLA) aggregation, each of which has its own characteristic dynamics and produces aggregates with different fractal dimensions d_f. We show here that the cluster-mass distributions are also markedly different, with $N(m)$ for DLA exhibiting a reasonably well-defined peak, while for RLA it is more nearly described as a power law. Furthermore, we show that the cluster-mass distributions exhibit dynamic scaling in both cases, and we suggest the appropriate form of the kernels for a Smoluchowski-equation description of the dynamics.

We measure $N(m)$ by analyzing transmission electron microscope (TEM) images of the clusters on TEM grids prepared at several times as the aggregation proceeds.[3] A sampling of the clusters is obtained from several low-magnification micrographs of random regions on a grid. The mass m_i of every cluster in the micrograph is determined by counting of the number of gold particles in the cluster i. Sufficient clusters are counted to obtain a representative sampling of $N(m)$ at each time, and the data are compiled in histograms, whose bins are divided evenly on a logarithmic scale, with the results normalized by the bin width. Thus the accuracy with which we must measure the cluster mass is reduced as the mass increases. While this measurement technique provides somewhat limited statistical accuracy, it is simple and provides results over a very large range of cluster masses.

Typical TEM images showing clusters produced in each regime are shown in Fig. 1. Initially, the colloid is stabilized against aggregation by the large charge on the surface of the particles, and by controllable reduction of this charge to varying degrees aggregation is induced with a wide range of rates. In Fig. 1(a) the clusters were produced by DLA, and the sample was prepared one minute after the aggregation was initiated. Since all the charge has been displaced, the clus-

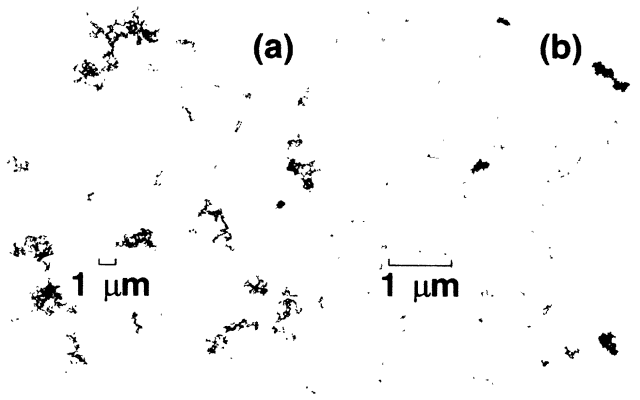

FIG. 1. Typical TEM images of clusters formed by (a) diffusion-limited aggregation and (b) reaction-limited aggregation. The aggregate's fractal dimensions and the cluster-mass distributions are clearly different for the two regimes.

ters stick to each other immediately upon collision, and the aggregation rate is limited solely by diffusion. The screening of the cluster interior due to the diffusive trajectory leads to the open, tenuous structure evidenced in the figure, with $d_f \approx 1.75$. Furthermore, while there is a broad distribution of cluster masses, no one size predominates. In contrast, Fig. 1(b) shows clusters produced by RLA, and was prepared two hours after the aggregation was initiated. The slow rate is a consequence of the remaining surface charge, which provides a Coulombic repulsion between the particles and results in a very low probability of sticking upon collision. Thus the diffusive trajectory no longer affects the cluster structure, but rather they can interpenetrate to a greater extent, leading to the denser structures evidenced by the larger clusters in the figure, and consistent with the higher fractal dimension $d_f \approx 2.05$. Furthermore, the cluster-mass distribution is clearly substantially different, as evidenced by the preponderance of clusters with very small masses.

A histogram analysis of the cluster-mass distribution for DLA is shown in a logarithmic plot in Fig. 2 for data collected three different times after the initiation of the aggregation. Each data set is normalized to the total number of single gold particles actually counted, $S_1 = \sum_i m_i N(m_i)$. As time increases, the number of clusters of a given mass decreases, while the mass of the largest clusters increases. The sample error bars shown reflect the statistical errors due to the number of clusters counted, normalized by the bin width. At the later times most of the bins at low mass contain, at most, only one cluster each. Empty bins are shown by the points below the axis break, while bins containing single clusters have the very large error bars.

The histograms of the cluster mass distributions for reaction-limited aggregation are shown in a logarithmic

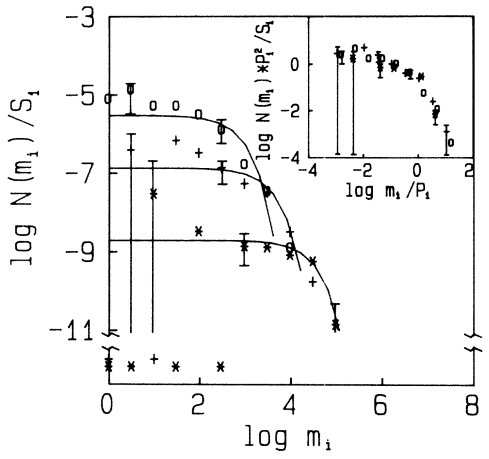

FIG. 2. Histogram analysis of the cluster mass distributions for DLA for samples prepared one minute (squares), ten minutes (plusses), and thirty minutes (asterisks) after the aggregation was initiated. The points below the break of the y axis represent empty histogram bins in the logarithmic plot, while the very large error bars reflect bins containing only one cluster each. Over 100 clusters, comprising $\sim 10^5$ gold balls, are included in each of the first two data sets, while 25 clusters, comprising $\sim 5\times 10^5$ gold balls, are included in the last. The data in the inset have been normalized with P_1 to show the dynamic scaling. The empty bins have not been included.

plot in Fig. 3, again for three different times after the aggregation is initiated. Each data set is again normalized by S_1. The data can be approximately characterized as a power law, $N(m) \sim m^{-\tau}$, up to some cutoff mass, which increases with time, and with $\tau = 1.5 \pm 0.1$.

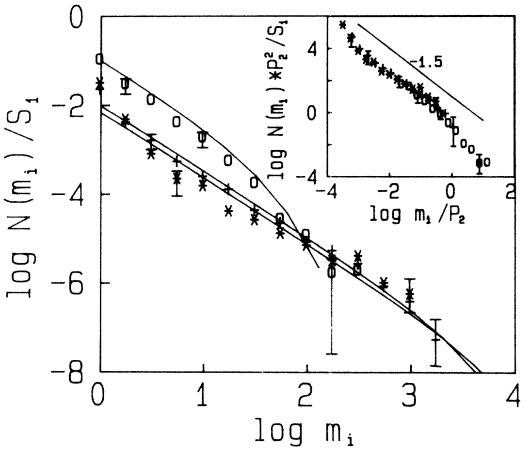

FIG. 3. Histogram analysis of the cluster-mass distributions for RLA for samples prepared two hours (squares), six hours (pluses), and eight hours (asterisks) after the aggregation was initiated. About 500 clusters are included in each data set. The data in the inset have been normalized with P_2 to show the dynamic scaling.

We use the Smoluchowski equations[8] to describe the time evolution of the cluster-mass distribution:

$$\frac{dN(m_i)}{dt} = \frac{1}{2}\sum_{j=1}^{i-1} K_{j,i-j}N(m_j)N(m_{i-j}) - \sum_{j=1}^{\infty} K_{i,j}N(m_i)N(m_j),$$

where $K_{i,j}$ is the kernel. In discussing solutions to the Smoluchowski equations, we define the nth moment of the distribution, $P_n = S_n/S_{n-1}$, where $S_n = \sum_i m_i^n N(m_i)$. If the solution exhibits dynamic scaling, it can be expressed as[11] $N(m_i,t) = P_n^{-2}\psi(m_i/P_n)$, where $\psi(x)$ is the scaling function whose form is time independent. Here P_n is any moment of the distribution which reflects the time dependence, which in turn can be characterized by a dynamic exponent[12,13] z, where $P_n \sim t^z$. Physically, a scaling solution implies that the distribution function attains a form whose shape is independent of time, while all the time dependence is reflected in the behavior of the moments of the distribution.

Many types of aggregation can be described with a class of homogeneous kernels which are characterized by $K_{i,j} \sim m_i^{\mu} m_j^{\nu}$, for $m_j >> m_i$ and $K_{ai,aj} = a^{\lambda}K_{i,j}$, so that $\lambda = \mu + \nu$. The solutions can be divided into several classes,[11] depending on the values of the exponents λ and μ, each exhibiting dynamic scaling, with a characteristic behavior both for the shape of the cluster mass distribution and its time evolution. Thus we can use our measured $N(m)$ to attempt to identify the class of the solution and hence the form of the kernel.

We first consider the appropriate kernel for diffusion-limited aggregation, which has traditionally been taken as[8,14] $K_{i,j} = 4\pi\sigma_{ij}(D_i + D_j)$, where D_i is the diffusion constant of a cluster of mass m_i and σ_{ij} is the effective collision radius for clusters of mass m_i and m_j. As a consequence of the screening,[2] we take $\sigma_{ij} = R_i + R_j$, where R_i is the radius of a cluster of mass m_i. Furthermore, scaling arguments,[15] as well as numerical solutions of the hydrodynamic equations,[16] suggest that $D_i \sim R_i^{-1}$. Thus, $K_{ij} \sim 2 + (m_i/m_j)^{1/d_f} + (m_j/m_i)^{1/d_f}$. We note that this is a special form of the class of kernels we are considering, with $\lambda = 0$ and $\nu = -\mu = 1/d_f$ (class III).[11] An analytic solution to the Smoluchowski equations does not exist for this kernel. However, except far off the diagonal, when $m_i << m_j$, this kernel is well represented by a constant, for which an analytic solution does exist,[17] $N(m_i) = S_0/P_1 \times (1 - 1/P_1)^{i-1}$. The solid lines in Fig. 2 represent the calculated distribution functions using the values obtained for S_0 and P_1 directly from the TEM analysis. The agreement with the data is satisfactory, except at small mass and long time.

To look for dynamic scaling, we have normalized each data set by P_1^2/S_0 and have plotted them as a function of m_i/P_1 in the inset in Fig. 2. Dynamic scaling is indeed observed, as all the data lie on a single curve, which in fact represents the shape of the scaling function $\psi(x)$. If the empty histogram bins had been included in the inset, $\psi(x)$ would tend toward zero at small x. The time dependence of P_1 is best described as a linear function of time, in accordance with quasielastic light-scattering measurements[18] which suggest that $z \approx 1$, as predicted by the constant kernel solution.[17]

The poor agreement between the analytic solutions and our data at low mass and long times most likely reflects the effects of the very large reaction rate far off the diagonal, where the approximation of a constant for the kernel fails badly. Physically, this large reaction rate is due to the small clusters with very large diffusion constants reacting with the large clusters with their large capture radii. This large off-diagonal term can be expected to lead to a faster depletion of the concentration of the small clusters. In fact, consistent with our observations, a decrease in the number of particles at low mass and long times has been predicted for aerosols,[19] as well as by a scaling analysis of the Smoluchowski equations.[11,13]

We now turn our attention to the data for RLA. The observation of a power-law cluster-mass distribution, with $\tau \approx 1.5$, immediately rules out a gelling kernel, with $\lambda > 1$, since this invariably results in a power-law distribution with $\tau \geq 2$. Furthermore, it excludes kernels with $\mu < 0$ (class III), since these result in a peaked cluster-mass distribution. Kernels with $\mu > 0$ (class I) can produce power-law solutions, and require $\lambda = 0.5$ to give $\tau = 1.5$ at the early stages of aggregation. Similarly, kernels with $\mu = 0$ (class II) can also produce power-law solutions with $\tau = 1.5$, but are, in general, more difficult to characterize. However, Ball[20] has proposed a geometric scaling model which suggests that the appropriate kernel has $\mu = 0$ and $\lambda = 1$, which not only results in a power-law solution with $\tau = 1.5$, but also predicts that the characteristic cluster size grows exponentially in time, in accordance with quasielastic light-scattering measurements for RLA.[5] For monodisperse initial conditions, an analytic solution exists for the sum kernel, $K_{i,j} \sim m_i + m_j$, which has similar scaling. In fact, this kernel was found to describe the cluster-mass distributions measured, for $i \leq 40$, for antigen-antibody–induced RLA of polystyrene colloids.[21] The solid lines in Fig. 3 are a fit to the sum kernel solutions

$$N(m_i) = S_1 e^{-ib}(m_i b)^{i-1}/P_1 m_i!,$$

where $b = 1 - 1/P_1$, and demonstrate good agreement with our data.

To investigate dynamic scaling for the RLA data, we

must use P_2 or a higher moment to reflect the time dependence of the distribution. We obtain P_2 by integrating the sum kernel prediction using the fitted values of P_1 for each data set. We have plotted the three data sets, each normalized by P_2^2/S_0, as a function of m_l/P_2 in the inset. The data all lie on a single curve, illustrating the dynamic scaling, and the shape of the curve represents $\psi(x)$. The time dependence of P_2 is exponential, in accordance with quasielastic light-scattering measurements.[5] Thus, z is not well determined here.

While the sum kernel solutions describe our data rather well at early times, the agreement is not as good for the data sets measured at long times. In fact, here our data might be described by two exponents, a larger one at small mass, and a smaller one at large mass. Indeed, such behavior is predicted[11] by the scaling analysis of the Smoluchowski equations for class-I kernels that are on the border of class II, having μ slightly greater than zero. Here, $N(m_l,t)$ is predicted to behave as for $\mu=0$ for an extended period of time, before reaching the steady-state solution, which has two distinct power-law regimes, with $\tau=1+\lambda$ at low mass and $\tau=\lambda$ at higher mass, until it is cut off exponentially. Furthermore, the dynamic exponent predicted is $z=1/(1-\lambda)$, which is very large for $\lambda\leq 1$, and, in practice, may not be distinguishable from the exponential growth measured. Thus, we conclude that the kernel which describes RLA is consistent with $\mu\geq 0$ and $\lambda\leq 1$, and thus may be either a class-II kernel or a class-I kernel that is very nearly class II.

In conclusion, we emphasize that all of these results were obtained with exactly the same colloid system. We merely changed the rate of aggregation by adjusting the surface charge on the particles. Nonetheless, we obtain two markedly different distribution functions, depending on the kinetics.

We thank Robin Ball, Max Kolb, and Tom Witten for many useful and enlightening discussions and John Dunsmuir for taking the TEM micrographs.

[a]Also at Department of Physics, City College of the City University of New York, New York, NY 10031.

[1]*Kinetics of Aggregation and Gelation,* edited by F. Family and D. P. Landau (Elsevier, Amsterdam, 1984).

[2]T. A. Witten and L. M. Sander, Phys. Rev. Lett. **47**, 1400 (1981).

[3]D. A. Weitz and M. Oliveria, Phys. Rev. Lett. **52**, 1433 (1984).

[4]D. W. Schaefer, J. E. Martin, P. Wiltzius, and D. S. Cannell, Phys. Rev. Lett. **52**, 2371 (1984).

[5]D. A. Weitz, J. S. Huang, M. Y. Lin, and J. Sung, Phys. Rev. Lett. **54**, 1416 (1984).

[6]P. Meakin, Phys. Rev. Lett. **51**, 1119 (1983); M. Kolb, R. Botet, and R. Jullien, Phys. Rev. Lett. **51**, 1123 (1983).

[7]R. Jullien, M. Kolb, and R. Botet, J. Phys. (Paris) Lett. **45**, L211 (1984).

[8]M. Von Smoluchowski, Phys. Z. **17**, 593 (1916).

[9]M. Kolb, Phys. Rev. Lett. **53**, 1653 (1984).

[10]R. Botet and R. Jullien, J. Phys. A **17**, 2517 (1984).

[11]P. G. J. Von Dongen and M. H. Ernst, Phys. Rev. Lett. **54**, 1396 (1985).

[12]T. Vicsek and F. Family, Phys. Rev. Lett. **52**, 1669 (1984).

[13]P. Meakin, T. Vicsek, and F. Family, Phys. Rev. B **31**, 564 (1985).

[14]S. Chandrasekhar, Rev. Mod. Phys. **15**, 1 (1943).

[15]P. G. de Gennes, *Scaling Concepts in Polymer Physics* (Cornell Univ. Press, Ithaca, NY, 1979).

[16]P. Meakin, Z. Y. Chen, and J. M. Deutch, J. Chem. Phys. **82**, 3786 (1985).

[17]R. J. Cohen and G. B. Benedek, J. Phys. Chem. **86**, 3696 (1982).

[18]D. A. Weitz, J. S. Huang, M. Y. Lin, and J. Sung, Phys. Rev. Lett. **53**, 1657 (1985).

[19]S. K. Friedlander and C. S. Wang, J. Colloid Interface Sci. **22**, 126 (1966).

[20]R. C. Ball, D. A. Weitz, T. A. Witten, and F. Leyvraz, to be published.

[21]G. K. Von Schulthess, G. B. Benedek, and R. W. DeBlois, Macromolecules **13**, 939 (1980).